Construction and Building Materials 158 (2018) 75–83

Contents lists available at ScienceDirect

Construction and Building Materials

journal homepage: www.elsevier.com/locate/conbuildmat

Nano-mechanical properties of alkali-silica reaction (ASR) products in concrete measured by nano-indentation

Chuanlin Hu [a,b], Bishnu P. Gautam [b], Daman K. Panesar [b,*]

[a] State Key Laboratory of Silicate Materials for Architecture, Wuhan University of Technology, Wuhan, China
[b] Department of Civil Engineering, University of Toronto, Toronto, ON, Canada

HIGHLIGHTS

- Nano-indentation and SEM analysis identified two ASR products (i) rosette-like (with crystalline characteristics), and (ii) granular (with amorphous characteristics).
- There is slightly lower Ca/Si and hardly any Na in the rosette-like ASR product compared to the granular ASR product.
- Nearly equal K/Si ratios are observed in the rosette-like and granular phases.
- Elastic modulus varied from 13.7 to 42.7 GPa (average = 27.4 GPa) for the rosette-like phases.

ARTICLE INFO

Article history:
Received 14 June 2017
Received in revised form 27 September 2017
Accepted 2 October 2017

Keywords:
Concrete
Alkali-silica reaction
Nano-mechanical properties
Nanostructure

ABSTRACT

This paper presents a study on the nano-mechanical properties of alkali-silica reaction (ASR) products formed in laboratory-prepared concrete specimens. The nano-mechanical properties (elastic modulus and hardness) of the ASR products were investigated by nano-indentation, and scanning electron microscopy (SEM) was used to investigate the corresponding material phases. The combined nano-indentation and SEM analysis identified two types of ASR products with distinct morphologies and compositions: a rosette-like ASR product and a granular ASR product. The nano-mechanical properties obtained from the nano-indentation tests were correlated with the two nanostructural morphologies. The findings provide insight into the correlation between nano-mechanical properties and nanostructure and improve our fundamental understanding of the mechanical behavior and durability of ASR-affected concrete.

1. Introduction

Alkali-silica reaction (ASR) is a deleterious chemical reaction between various metastable forms of silica contained in aggregate particles and the alkali and hydroxyl ions in the pore solution of hydrated cement [1]. When incorporated with water, the hydrophilic reaction product is expansive and may cause severe and irreversible expansion, cracking, and degradation of the mechanical properties of concrete [1]. The implications of ASR are seen worldwide in concrete structures including dams, power plants, and transportation and building infrastructure [2]. Ensuring the safety of ASR-affected structures requires evaluating the effects of ASR on the mechanical behavior and durability of concrete.

Several studies have focused on the ASR-induced degradation of mechanical properties by testing laboratory specimens and core samples from field structures [3,4]. Recently, Esposito et al. reviewed several studies on the effects of ASR on the mechanical properties of concrete [5]. However, the degradation of mechanical properties is caused primarily by the cracking of aggregate caused by ASR; hence, the study of ASR-related cracking is essential to obtain mechanistic insights into the degradation of mechanical properties.

Both surface cracks and micro-cracks inside concrete have been monitored as a means of assessing damage to concrete caused by ASR [6–10]. Attempts have been made to interpret the loss of mechanical properties based on the extent and orientation of cracks [3,11,12]. Gautam and Panesar assessed the micro cracking, microstructure, and mechanical properties of ASR-affected concrete and found that the evolution of the mechanical properties of ASR-affected concrete is governed not only by the formation of micro-cracks as a result of ASR, but also by the mineralogy and morphology of the ASR products in the aggregate and paste cracks that evolve over time [12]. Since the mechanical properties of concrete are affected by both the ASR cracks and the characteristics of the ASR products, the effects of ASR on the evolution of the

* Corresponding author.
E-mail address: d.panesar@utoronto.ca (D.K. Panesar).

https://doi.org/10.1016/j.conbuildmat.2017.10.006
0950-0618/

mechanical properties of concrete can be further understood by evaluating the mechanical properties of the ASR products and associated concrete micro/nano-structures.

Over the past several decades, numerous studies have examined the reaction mechanism and microstructure of ASR products [13–24]. However, few studies have closely examined the mechanical properties of ASR products on the micro/nano-scale [25,26]. Leemann and Lura used micro-indentation to study the mechanical properties of crystallized ASR products in a sample from a 45-year-old bridge in Switzerland [25]. Zheng et al. studied the mechanical properties of a synthesized ASR product in a simplified calcium-alkali-silicate system using nano-indentation [26]; however, that study was limited to the synthesized product and highlighted the need to extrapolate the findings to field structures affected by ASR. This study aims to improve the fundamental understanding of the nano-mechanical properties of ASR products formed in ASR-affected concrete. The ASR gel formed within cement paste is generally intermixed with the cement hydration products (mainly C—S—H gel), which influences the nano-mechanical properties of ASR products. Therefore, this study investigates ASR products formed inside aggregate cracks. This study estimates the nano-mechanical properties of ASR products with various morphologies and correlates them with the nanostructures of the ASR products, which is helpful to understand the effects of ASR on the mechanical behavior and durability of concrete.

2. Materials and methods

2.1. Materials and mix proportions

General use (GU) high-alkali cement was used to prepare the concrete specimens (see Table 1 for the chemical compositions). The concrete mix was designed according to the standard ASTM C1293 [27], and the components of the mix are shown in Table 2. The alkali content of the concrete was increased to 5.25 kg Na_2O equivalent per cubic meter of concrete by dissolving alkali pellets (sodium hydroxide) in the mixing water. Non-reactive natural sand from Orillia, Ontario, Canada was used as the fine aggregate. Reactive siliceous limestone aggregate from Ontario, Canada (Spratt aggregate) was used as the coarse aggregate. As the reaction mechanism of alkali and silica is closely related to the type of aggregate [28], the compositions of the aggregates used in this study were characterized by the X-ray diffraction (XRD). As shown in Fig. 1, the XRD patterns of the aggregates show that the sand was composed mainly of quartz, whereas the coarse aggregate was composed mainly of calcite with small amounts of ankerite and silicate.

2.2. Concrete specimens and sample preparation

The concrete samples for this study were taken from cylinder specimens with dimensions of 100 × 200 mm cast with the reactive concrete mix. During specimen preparation, fresh concrete was first mechanically mixed and then cast into plastic cylinder molds. The molds were removed after one day, and the specimens were then cured in a fog room at a temperature of 23 ± 3 °C and covered with wet burlap and a plastic sheet for six months. After six months, the specimens were conditioned in an environmental chamber maintained at a temperature of 50 ± 0.5 °C with relative humidity >95% for one year. A previous study indicated that the expansion potential of the specimens was exhausted by one year of conditioning [12].

To prepare the thin sections for nano-indentation tests and subsequent SEM analysis, a concrete sample with a thickness of approximately 10–20 mm was cut out from the middle portion of the cylindrical specimen and impregnated with low-viscosity epoxy. The procedure for the preparation of the thin section included cutting, immersion in epoxy resin, grinding, and polishing (see Ref. [29] for the detailed procedure of thin-section preparation). Finally, to achieve a smooth surface, the thin section was successively polished by oil-based suspensions (9-, 3-, 1-, and 0.25-μm grit). At the end of each polishing step, the thin section was cleaned with kerosene in an ultrasonic bath, and the surface was then examined using an optical microscope. After polishing, the thickness of the thin section was >50 μm, which is thick enough for nano-indentation tests as the maximum penetration depth of the nano-indentation tip is on the order of several hundred nanometers.

Table 2
Mix proportion for the preparation of ASR concrete.

Constituents	Cement	Coarse aggregate	Fine aggregate	Water	Alkali pellet
Mass (kg/m^3)	420.0	1115.0	719.2	184.8	1.41

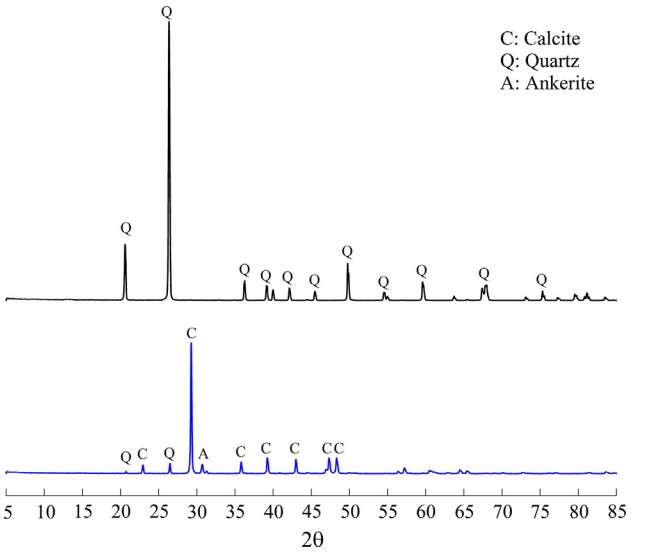

Fig. 1. XRD patterns of fine aggregate (top) and siliceous limestone coarse aggregate (bottom).

2.3. Nano-indentation analysis

A hardness tester equipped with a Berkovich tip was used for the nano-indentation tests of the thin sections. A typical load–depth (P–h) curve generated from a nano-indentation test of an ASR product is shown in Fig. 2. The elastic modulus E and hardness H were obtained from the slope of the unloading process in the P–h curve using Eqs. (1) and (2), respectively [30]:

$$E = \frac{(1-\upsilon^2)}{2}\sqrt{\frac{\pi}{A}}\frac{dP}{dh}\Big|_{h=h_{max}}, \quad \text{and} \tag{1}$$

$$H = \left(\frac{P}{A}\right)\Big|_{h=h_{max}}, \tag{2}$$

where υ is the Poisson's ratio of the indented material nanostructure, A is the contact area, which can be calculated from the indentation depth h using the Oliver–Pharr method [31], and h_{max} is the maximum indentation depth. In this study, the Poisson's ratio of the nanostructure was assumed to be 0.18 [25]. Four maximum loads were applied (4, 6, 8, and 10 mN), and the corresponding loading rates of 8, 12, 16, and 20 mN/min were used to achieve the same loading history with a 30-s loading process from zero to the maximum load and a 30-s unloading process from the maximum load to zero.

2.4. Scanning electron microscopy (SEM) analysis

After the nano-indentation tests, the thin section was coated with carbon and investigated by SEM (complemented by an energy-dispersive spectrometer). Backscattered electron (BSE) images were taken at different magnifications to study the distributions and morphologies of the material nanostructures, and energy-dispersive X-ray spectroscopy (EDX) elemental analysis was performed to characterize the chemical compositions of the material nanostructures corresponding to the nano-indentation tests. The number of counts for a test duration of

Table 1
Chemical composition of GU cement.

Constituents	LOI	SiO_2	Al_2O_3	Fe_2O_3	CaO	MgO	SO_3	Alkali	Free Lime	Insoluble
Mass%	2.27	19.25	5.33	2.41	62.78	2.36	4.01	0.99	1.29	0.52